SDC-92-299

SDC
SOLENOIDAL DETECTOR NOTES

RESPONSE TO CONCERNS OF THE EM REVIEW COMMITTEE

August 1, 1992

Norman F. Hill, Victor Guarino and James Nasiatka
Argonne National Laboratory

The submitted manuscript has been authored by a contractor of the U. S. Government under contract No. W-31-109-ENG-38. Accordingly, the U. S. Government retains a nonexclusive, royalty-free license to publish or reproduce the published form of this contribution, or allow others to do so, for U. rnment purposes.

ANL-HEP-TR-92-67
SDC-92-299

Response to Concerns of the EM Review Committee*

Norman F. Hill, Victor Guarino, and James Nasiatka

High Energy Physics Division, Argonne National Laboratory
Argonne, Illinois 60439

01 August 1992

Introduction

During the technical review of the stacked versus cast Electromagnetic Calorimeter on June 24 at the SSC Laboratory, certain questions were raised about the technical reliability of the cast lead EMC. The committee asked for specific response to the following concerns:

1. Deflections resulting from a structure weakened to accommodate longer shower maximum η strips.
2. Assembly plans and scenarios considering the deflections as outlined in question 1.
3. Compatibility with shower max.
4. Positioning of source tubes.
5. Subsequent to the last review an additional question has been raised about stress levels in the lead/bulkhead connections.

We will present responses to each of these questions, and are prepared to answer any additional questions the committee may raise.

* Work supported by the U.S. Department of Energy, Division of High Energy Physics, Contract W-31-109-ENG-38.

Deflections

The cast lead SDC EMC module was designed using Finite Element methods to minimize the amount of dead material in the module and yet provide a structurally stable unit. The original module was a 1/64th (azimuthal) wedge and is shown in Fig. 1. The finite element model was constructed using shell elements to model the individual lead plates, the bulkheads and the 1/8" stainless steel frame. The model was fully constrained along the back where the EM section is attached to HAD-1. The model was gravitionally loaded and analyzed in both 12 o'clock and 3 o'clock positions. The FEA model was stepped along the back where the EM would mate with the HAD-1; however the shower max cell was not stepped but was instead a continuous cell that ran parallel to the beam line. Shower max was located 6 cells back from the front plate. This module design was optimized from a physics perspective because it minimized the amount of dead material in the structure. However at the time of the June review, the lack of structural material caused by recent enlargement of the shower max slot produced deflections which were unacceptable. The maximum deflections were produced when the module was hung in the 12 o'clock position. In this position the individual lead plates, which were suspended between bulkheads at $\eta = .2$, deflected radially inward at $\eta = .1$.

The deflections of the lead plate as described, occurred because of the natural deflection of a plate suspended over the designed span. This deflection is caused by the weight of the lead and the deflection of the module frame. The maximum deflection of the frame occurred where η equals 1.4 at the front plate. The frame was displaced by 1.69 mm in the beam direction and by 5.12 mm radially inward. The maximum deflection in the lead plates occurred in the last tower between the bulkheads at $\eta = 1.2$ and the endplate at $\eta = 1.4$ in front of shower max and was 4.9 mm radially inward. This maximum deflection of the lead plate occurred at the bulkhead which does not penetrate shower max at $\eta = 1.3$.

It was concluded that two modifications were needed to reduce these deflections:

- **A)** Not allowing the front plate to move in the beam direction, and
- **B)** Stiffening the front plate .

A) Fixing the Front Plate at Z = 0

As a first step, the FEA model was run with the front plate restrained from moving in the beam direction by fixing the intersection of the end and front plates at the Z = 0 end. Figure 2, Case 1 shows a cross sectional view of the module and the boundary conditions under which it was run. Once again the maximum frame displacement occurred at the endplate at $\eta = 1.4$ along the front plate; however it was reduced to .093 mm in the beam direction and .183 mm radially inward from 2.69/5.12 mm, respectively. The maximum lead plate deflections occurred at the same point but were reduced from 4.9 to 3.7 mm radially inward. These deflections were still unacceptably high.

Up to this point a Youngs Modulus for pure lead (2×10^6) had been used in all the analyses. To gain increased stiffness, it was concluded that a lead alloy should be used in the casting. Current tensile tests being done on the calcium-tin alloy have confirmed that a modulus of 3×10^6 would more accurately model the alloys we intend to use (see Fig. 3). The FEA model was again run with the front plate fixed at Z = 0 and the higher modulus lead alloy. Figure 4, Case 2 shows a cross sectional view of the model with the FEA parameters. The maximum lead plate deflections in this case were reduced from 3.7 mm in the previous case to 2.9 mm.

Westinghouse Science and Technology Center Results

In order to check the analytical methods used by ANL, we requested that WSTC duplicate the model and independently analyze the results. The results of this analysis are presented as written by D. Scherbarth.

It should be pointed out that this analysis was done using ANSYS, a much more sophisticated (more expensive) analytical software package than COSMAS M that has been used at Argonne. The analysis was done by a Westinghouse analyst, familiar with the program and its idiosyncrasies. Minor differences in the two models are described below.

1. The Westinghouse model incorporated the stepped shower maximum slot whereas the Argonne model, created much earlier, did not.
2. The model used straight rectangular plates for the bulkheads, whereas the Argonne model used the actual bulkhead shape.

The closest comparison to the Westinghouse model (Appendix A) is represented by Argonne's Fig. 4, Case 2 .

The maximum deflection of the lead was occurring in both Cases 1 and 2, and in the Westinghouse model at the same position. The bulkheads at η = .1 in front of the shower max slot offered little support to the lead. Therefore, it was decided to revisit a case in which all of the bulkheads penetrated the shower max slot, in order to reestablish a base line. Figure 5 (Case 3) illustrates a cross sectional view of the module and the conditions under which the third case was run. It found that the maximum lead plate deflection occurred in the lead plate immediately behind the shower max slot between the bulkhead at $\eta = 1.3$ and the endplate between 1.4 behind the shower max slot and was .447 mm.

B) Stiffened Front Plate

The next step was to add a stiffened front plate. It was concluded that if the front plate could be stiffened, the bulkheads would be further restrained. This step would also provide additional support to the lead, resulting in further reductions of the deflections.

As a first attempt at studying the effects of a stiffened front plate, a 1" aluminum plate was attached. Figure 6 (Case 6) represents that change. A lead modulus of 3×10^6 was used, the bulkheads penetrated the shower max slot at $\eta = .2$ and the front plate was fixed at Z = 0. This case produced a maximum lead plate deflection of .618 mm in plate 1. In order to reduce the mass, we then investigated attaching aluminum stiffeners (in place of a solid aluminum plate). This is shown in Fig. 7 as Case 9. In Case 9, five 1-mm aluminum stiffeners were run the length of the module, and the 1/8" front plate was bent down on one side only. In addition 1-mm thick transverse stiffeners were added at every bulkhead. This represents a low mass rigid structure. In Case 9 a lead modulus of 3×10^6 was used. The bulkheads penetrated the shower max slot at $\eta = .2$ and the front plate was fixed at Z = 0. The maximum lead plate deflection in Case 9 was .506 mm.

At this point in the analysis, it appeared that we had reduced the deflections to an acceptable level by stiffening the front plate. Further methods of reducing the deflections were explored. It was noted that the end plates bowed outward in the beam direction with the maximum bowing

occurring directly behind shower max. It was felt that if the end plate was fixed along its entire length, and not just at the front plate, the deflections might be reduced further. Figure 8 Case 10 illustrates the EM module, without any stiffening of the front plate. A lead modulus of 3×10^6 bulkheads penetrating the shower max slot at $\eta = .2$, and the endplate at $Z = 0$ was completely fixed along its length. These changes resulted in minimal improvement in the lead plate deflections, however the overall structural distortion was dramatically reduced.

Based on the results of these cases, we deduced that the ultimate solution to the lead plate deflections, that was acceptable from a physics perspective, would be to stiffen the front plate by bending the 1/8" plate downward and bonding a 1" thick plate of "Hexcel" to the front plate. Figure 9 shows Case 11 was run to simulate this structure. In Case 11 a new model was created representing a 1/32 azimuthal wedge. The model of the 1/32 module was identical to the 1/64th module but included a stepped shower max, and a single Hexcel plate joining the two 1/64th castings together at the front plate. Hexcel is a bonded structure and therefore is impossible to model accurately using Finite Elements. For that reason the stiffness of the Hexcel was approximated by an eggcrate structure composed of thin stiffeners running the length of the module and across the width of the module. The stiffness of the Hexcel was approximated by changing the thickness of the stiffeners to appropriate thicknesses. An eight foot long 1" thick piece of Hexcel was loaded in simple bending and the deflections then measured under increasing load. An FEA model of this same piece of Hexcel was then created using the equivalent stiffness. The thickness of the stiffeners was then iterated until the FEA model of the Hexcel displaced in the same manner as the Hexcel tested. In Case 11 the maximum lead plate deflection occurred in plate 3 in the last tower and was .608 mm. The range of deflections in the entire system is shown in Fig. 9.

Conclusions

In summary, the three steps taken subsequent to the June Review were:

1. Use increased lead modulus.
2. Stiffen front plate.
3. Fix 90° end of the module

The end result of incorporating these steps is shown in Fig. 9A as Case 11.

Handling and Assembly of the Cast Lead Electromagnetic Calorimeter

There is a concern during handling of the casting that deflections can distort or break scintillator plates. However, this can be dealt with quite easily by using a handling fixture that does not allow any Z axis movement. As a test of this premise, an FEA model was run with the module constrained at $\eta = 1.4$ end as opposed to constraining it at $\eta = 0$ end.

The results are shown in Table 1. It is evident when comparing the displacements, that constraining the module at either end produces essentially the same results.

The sequence of steps one might use during fabrication and assembly are as follows:

1. Removal from mold, Fig. 10.
2. Place on machine table and machine angled surface.
3. Remove from machine and transportation in position shown.
4. Place on flat surface and remove fixture.
5. Mount turning fixture Fig. 11A and rotate 180° and place back on flat surface with center line horizontal.
6. Using rough casting lift fixture place second casting on top of first.
7. Mount back joining plate and attach 1/32 lifting and rotating fixture Fig. 11B.
8. Rotate 90° and bond "Hexcel" to front surface joining to castings.
9. Use rotation/lift fixture to rotate 90° for mounting on hadron section.

Compatibility with Shower Max

Figures 12 through 15 represent a suggestion for construction of the shower max and the fiber routing that conform to the cast lead construction. Other methods have been suggested by the Saclay group, but models have not been evaluated. These are to be supplied for a wooden model now being constructed at Argonne and Fermilab.

Lead Plate Stresses at the Bulkhead Connections

A question has been raised at both the June Review meeting in Dallas and teleconference meetings since, about lead stresses at the bulkhead connections. We will respond to those concerns in this portion of this report.

In anticipation of this problem, we designed and built a simple one plate test mold that has been used and will be used in the future as a test bed for looking specifically at this issue. As a review of the calculated values we present the following:

$\eta = .1$

l = length = 419.1 mm = 16.5"

q = weight/length = .0917 N/mm

I = moment of inertia = 1099.73 mm^4 of cross section

$$y_{max} = \frac{ql^4}{384EI} = \frac{\left(.0917\ \frac{N}{mm}\right)(419.1mm)^4}{384\left(13.79 \times 10^3 \frac{N}{mm^2}\right)\left(1099.73mm^4\right)}$$

y_{max} = .486 mm = .019" (deflection at center of the span).

M = Bending moment @ bulkhead assuming a rigid connection

$$M = \frac{wl^2}{12} = \frac{\left(.0917\frac{N}{mm}\right)(419.1mm)^2}{12}$$

$$M = 1342.22 \text{ Nmm} = 11.88 \text{ in-lbs}$$

Using this bending moment, and fitting it to the curve obtained from tests performed on a single plate casting indicates that the failure mode is well above the calculated moments (see Fig. 16). It is evident that Finite element analysis cannot accurately model this construction. It is also evident that standard classical calculations do not accurately represent this construction. For this reason, we are suggesting that a conservative design be adopted and thoroughly tested. Figures 17 and 18 represent, what we feel is, that conservative design. This design can be tested using our single plate mold/test fixture. Some preliminary calculations, on tube strengths for this proposed design change, are shown in Figs. 19 and 20. By using laser punching techniques for perforations this modification can be achieved at a small cost increase.

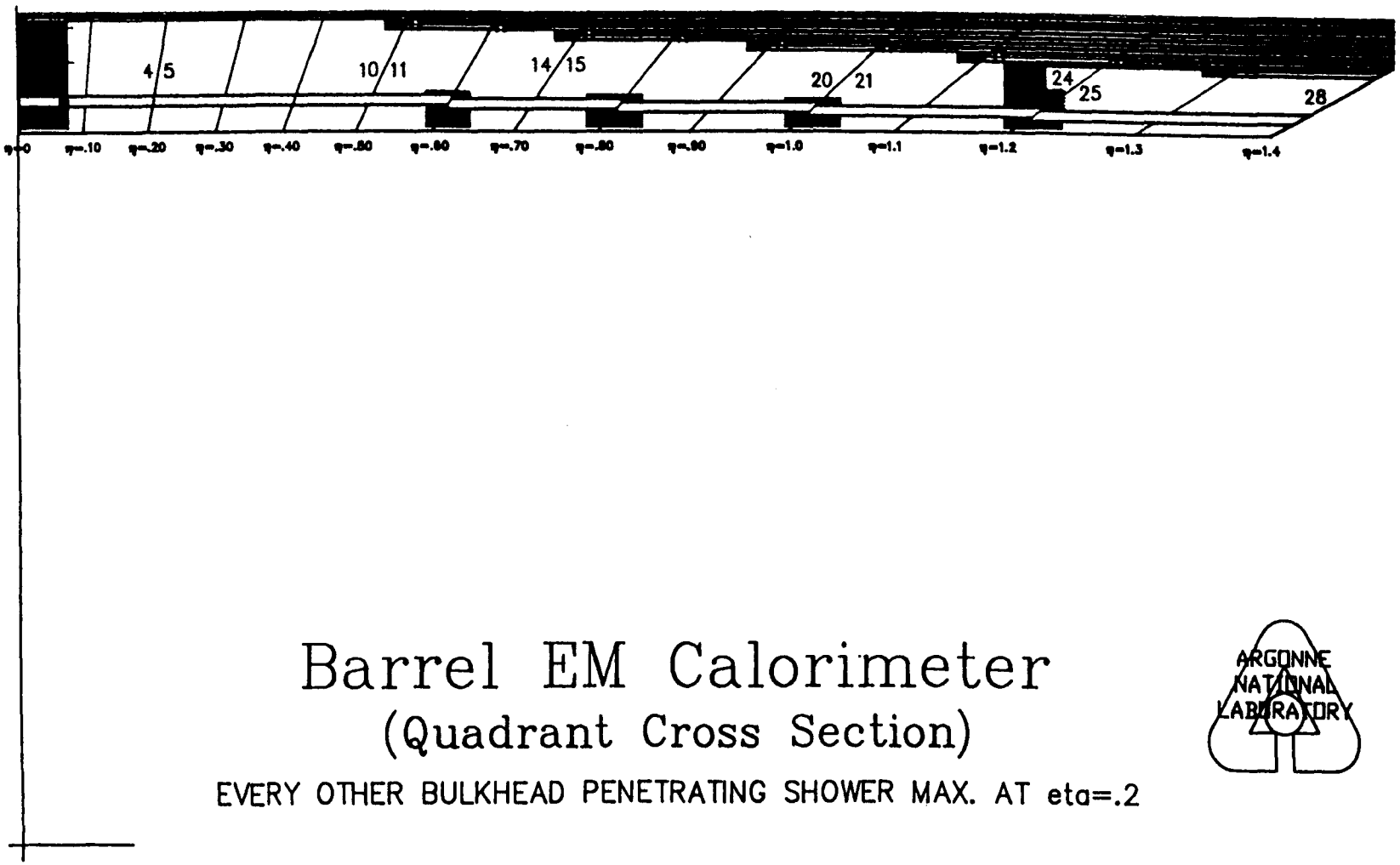
4
5
10
11
14
15
20
21
24
25
28
η=0
η=.10
η=.20
η=.30
η=.40
η=.50
η=.60
η=.70
η=.80
η=.90
η=1.0
η=1.1
η=1.2
η=1.3
η=1.4
Barrel EM Calorimeter
(Quadrant Cross Section)
EVERY OTHER BULKHEAD PENETRATING SHOWER MAX. AT eta=.2
ARGONNE
NATIONAL
LABORATORY

Figure 1

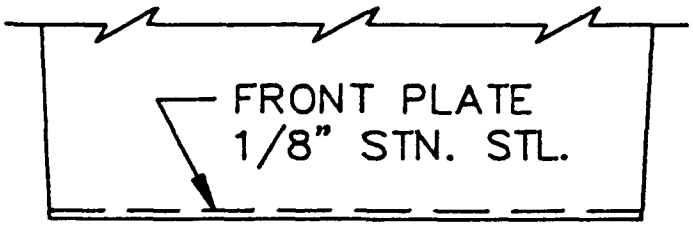

Case-1

PURE LEAD MODULUS: 2,000,000 PSI
EVERY OTHER BULKHEAD PENETRATING SHOWER MAX. AT eta = .2
FRONT PLATE FIXED AT Z=0
64 MODULES/BARREL

Location		Bulkhead Displ.		Max. Lead Displ.		Cell Displ.		Case 1
ETA	Cell	ΔZ (mm)	Δr (mm)	ΔZ (mm)	Δr (mm)	ΔZ (mm)	Δr (mm)	
0-.2	1	.073	0	.141	- .581	.068	- .581	Max. frame stress = 11,900 psi
0-.2	7	.490	0	.502	- .115	.012	- .115	Max. bulkhead stress = 2,900 psi
1.2-1.4	1	.098	-.183	.160	-3.667	.062	-3.484	Max. lead stress = 696 psi
1.2-1.4	7	.539	-.834	.554	- 1.562	.015	- .728	in 4th lead plate at eta = 1.4

Figure 2

Stress – Strain Curves for L50737 Lead Alloy
.06% Ca .5% Sn

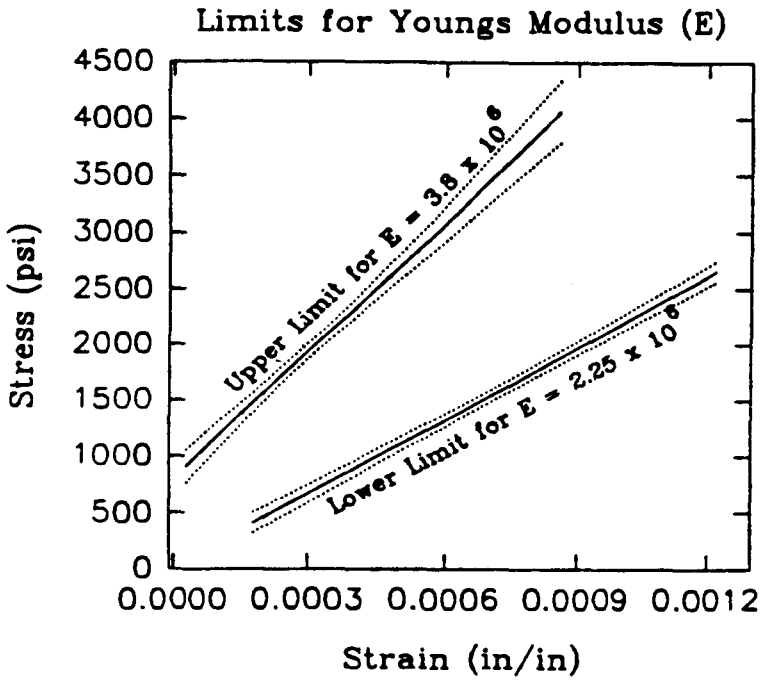

σ_y = 3,200 – 3,500 p.s.i

E = 3.05 x 10^6 p.s.i

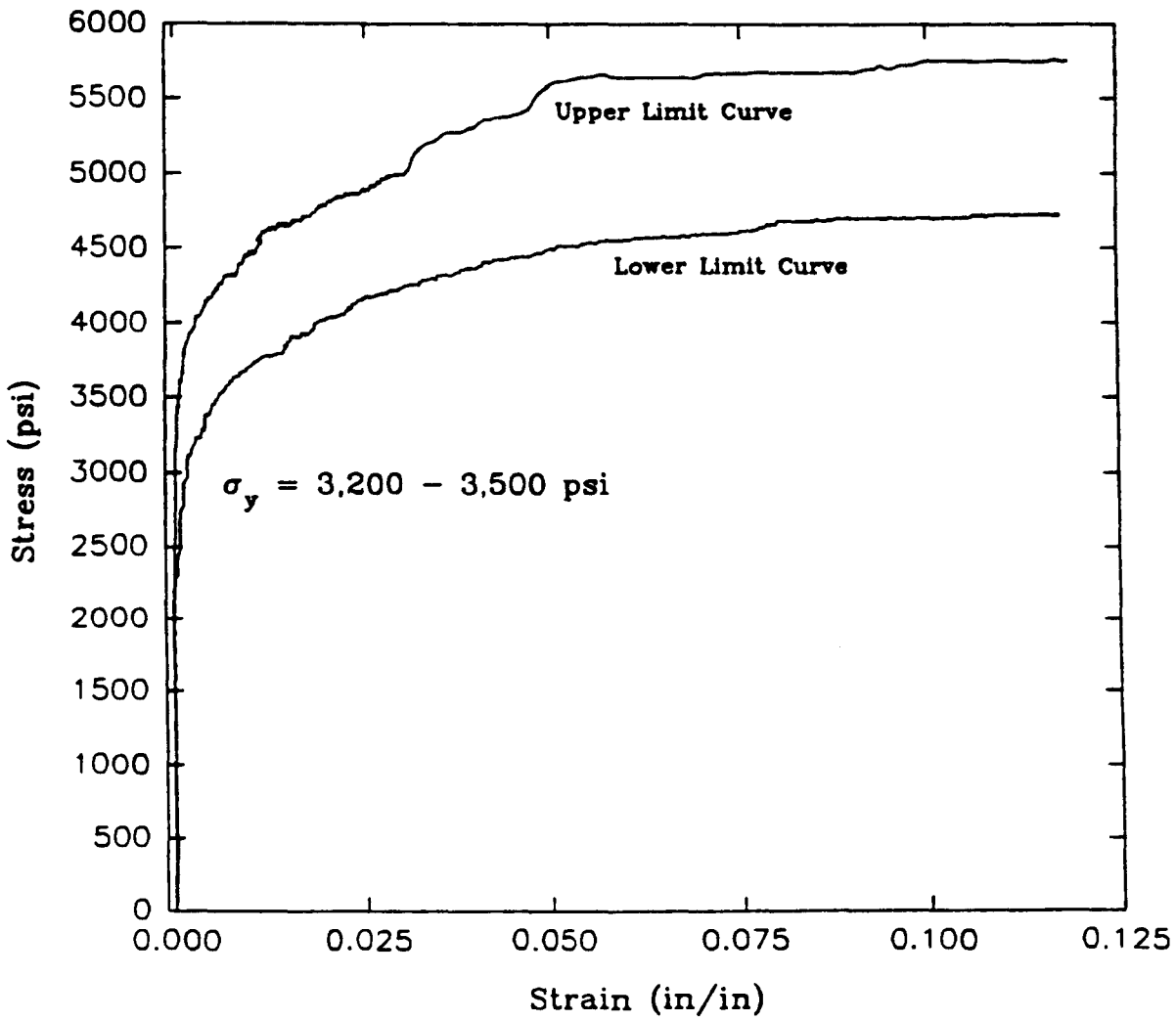

Figure 3

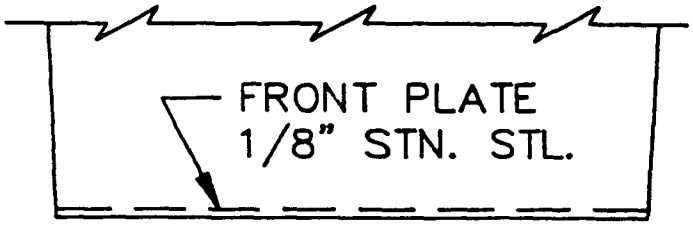

Case-2

LEAD ALLOY MODULUS: 3,000,000 PSI
EVERY OTHER BULKHEAD PENETRATING SHOWER MAX. AT eta = .2
FRONT PLATE FIXED AT Z=0
64 MODULES/BARREL

Location		Bulkhead Displ.		Max. Lead Displ.		Cell Displ.		Case 2
ETA	Cell	ΔZ (mm)	Δr (mm)	ΔZ (mm)	Δr (mm)	ΔZ (mm)	Δr (mm)	
0-.2	1	.068	0	.126	- .512	.058	- .512	Max. frame stress = 11,200 psi
0-.2	7	.443	0	.455	- .097	.012	- .097	Max. bulkhead stress = 2,500 psi
1.2-1.4	1	.095	-.172	.147	-2.951	.052	-2.779	Max. lead stress = 754 psi
1.2-1.4	7	.476	-.747	.488	-1.248	.012	- .501	in 2nd lead plate at eta = 1.4

Figure 4

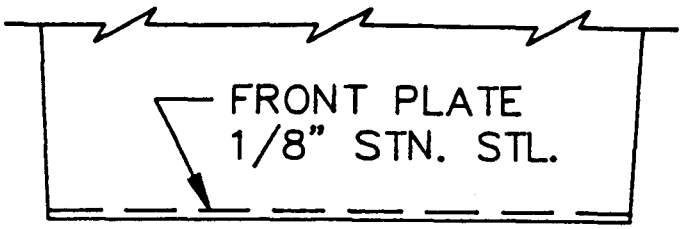

Case-3

LEAD ALLOY MODULUS: 3,000,000 PSI
EVERY BULKHEAD PENETRATING SHOWER MAX. AT eta = .1
FRONT PLATE FIXED AT Z=0
64 MODULES/BARREL

Location		Bulkhead Displ.		Max. Lead Displ.		Cell Displ.		Case 3
ETA	Cell	ΔZ (mm)	Δr (mm)	ΔZ (mm)	Δr (mm)	ΔZ (mm)	Δr (mm)	
0-.2	1	.070	-.018	.068	- .019	.002	- .001	Max. frame stress = 11,200 psi
0-.2	7	.450	-.090	.450	- .080	0	- .010	Max. bulkhead stress = 2,300 psi
1.2-1.4	1	.098	-.188	.098	- .447	0	- .259	Max. lead stress = 490 psi
1.2-1.4	7	.488	-.931	.487	-1.263	.001	- .332	in 3rd lead plate at eta = 0

Figure 5

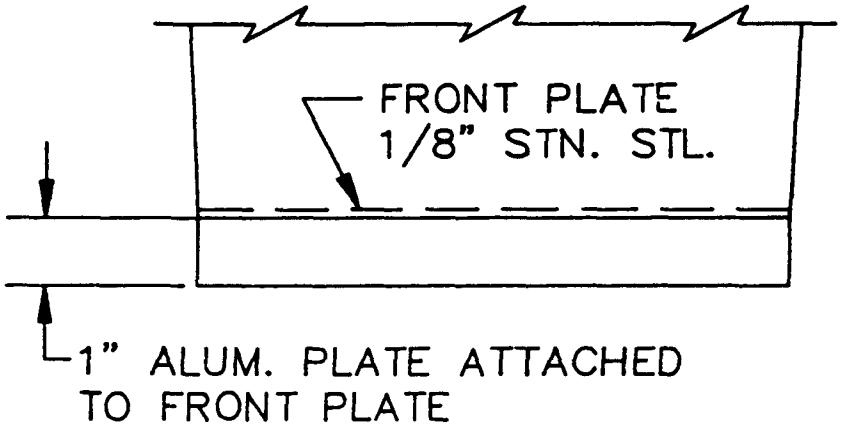

Case–6

LEAD ALLOY MODULUS: 3,000,000 PSI
EVERY OTHER BULKHEAD PENETRATING SHOWER MAX. AT eta = .2
FRONT PLATE FIXED AT Z=0
64 MODULES/BARREL

Location		Bulkhead Displ.		Max. Lead Displ.		Cell Displ.		Case 6
ETA	Cell	ΔZ (mm)	Δr (mm)	ΔZ (mm)	Δr (mm)	ΔZ (mm)	Δr (mm)	
0-.2	1	.074	-.022	.070	- .208	.004	- .186	Max. frame stress = 10,800 psi
0-.2	7	.406	-.088	.399	- .117	.007	- .029	Max. bulkhead stress = 2,700 psi
1.2-1.4	1	.050	-.081	.085	- .618	.035	- .537	Max. lead stress = 420 psi
1.2-1.4	7	.437	-.679	.452	-1.162	.015	- .483	in 3rd lead plate at eta = 1.4

Figure 6

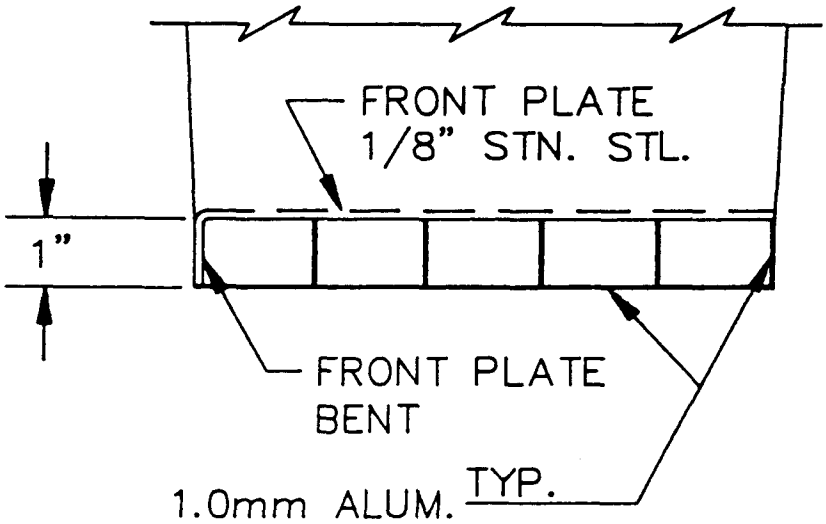

Case-9

LEAD ALLOY MODULUS: 3,000,000 PSI
EVERY OTHER BULKHEAD PENETRATING SHOWER MAX. AT eta = .2
FRONT PLATE FIXED AT Z=0
64 MODULES/BARREL

Location		Bulkhead Displ.		Max. Lead Displ.		Cell Displ.		Case 9
ETA	Cell	ΔZ (mm)	Δr (mm)	ΔZ (mm)	Δr (mm)	ΔZ (mm)	Δr (mm)	
0-.2	1	.044	-.017	.079	- .177	.035	- .160	Max. frame stress = 10,800 psi
0-.2	7	.408	0	.410	- .112	.002	- .112	Max. bulkhead stress = 2,000 psi
1.2-1.4	1	.067	-.031	.106	- .506	.039	- .475	Max. lead stress = 400 psi
1.2-1.4	7	.447	-.694	.461	-1.047	.014	- .353	in 3rd lead plate at eta = 1.4

Figure 7

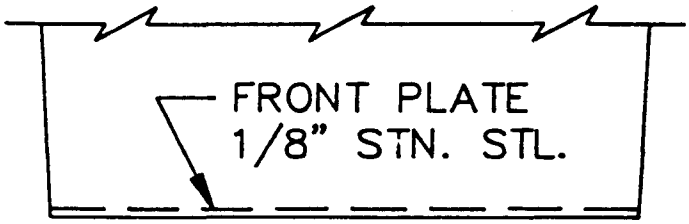

Case-10

LEAD ALLOY MODULUS: 3,000,000 PSI
EVERY OTHER BULKHEAD PENETRATING SHOWER MAX. AT eta = .2
END PLATE FIXED AT Z=0
64 MODULES/BARREL

Location		Bulkhead Displ.		Max. Lead Displ.		Cell Displ.		Case 10
ETA	Cell	ΔZ (mm)	Δr (mm)	ΔZ (mm)	Δr (mm)	ΔZ (mm)	Δr (mm)	
0-.2	1	0	0	.005	- .189	.005	- .189	Max. frame stress = 3,900 psi
0-.2	7	0	0	.009	- .029	.009	- .029	Max. bulkhead stress = 435 psi
1.2-1.4	1	.025	-.053	.027	-3.181	.002	-3.128	Max. lead stress = 600 psi
1.2-1.4	7	.056	-.104	.059	- .479	.003	- .375	in 2nd lead plate at eta = 1.4

Figure 8

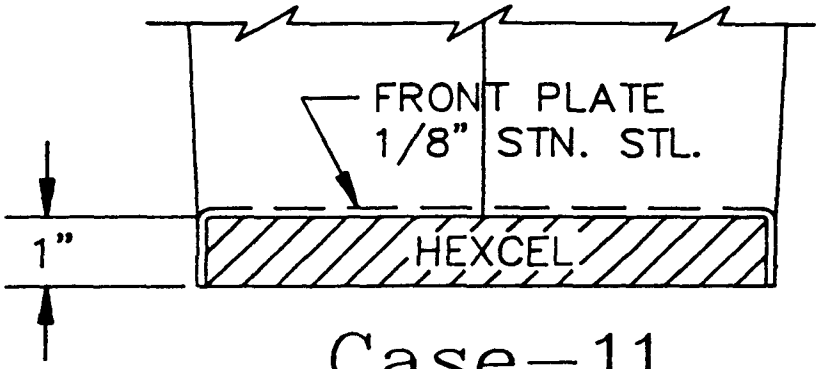

Case–11

LEAD ALLOY MODULUS: 3,000,000 PSI
EVERY OTHER BULKHEAD PENETRATING SHOWER MAX. AT eta = .2
END PLATE FIXED AT Z=0
32 MODULES/BARREL

Location		Bulkhead Displ.		Max. Lead Displ.		Cell Displ.		Case 11
ETA	Cell	ΔZ (mm)	Δr (mm)	ΔZ (mm)	Δr (mm)	ΔZ (mm)	Δr (mm)	
0-.2	1	0	0	.006	- .022	.006	- .022	Max. frame stress = 2,200 psi
0-.2	7	0	0	.016	- .022	.016	- .022	Max. bulkhead stress = 2,200 psi
.6-.8	1	.016	-.020	.027	- .071	.011	- .051	Max. lead stress = 246 psi
.6-.8	7	.011	-.015	.101	- .140	.090	- .125	in 3rd lead plate at eta = 1.4
1.2-1.4	1	.024	-.051	.040	-.334	.016	-.283	
1.2-1.4	3	.049	-.097	.119	-.705	.070	-.608	
1.2-1.4	8	.115	-.190	.127	-.672	.012	-.482	
1.2-1.4	18	.013	-.016	.019	-.284	.006	-.268	

Figure 9

Location		Bulkhead Displ.		Max. Lead Displ.		Cell Displ.		Case 12 Restrained at the high eta end
ETA	Cell	ΔZ (mm)	Δr (mm)	ΔZ (mm)	Δr (mm)	ΔZ (mm)	Δr (mm)	
0-.2	6	.040	0	.041	- .034	.001	- .034	Max. frame stress = 1,700 psi
0-.2	14	.038	0	.038	- .027	0	- .027	Max. bulkhead stress = 2,700 psi
1.2-1.4	1	0	-.003	.004	- .356	.004	- .353	Max. lead stress = 203 psi
1.2-1.4	3	0	-.003	.002	- .428	.002	- .425	in 3rd lead plate at eta = 1.4
1.2-1.4	18	.039	-.053	.039	-.351	0	-.298	

Table 1

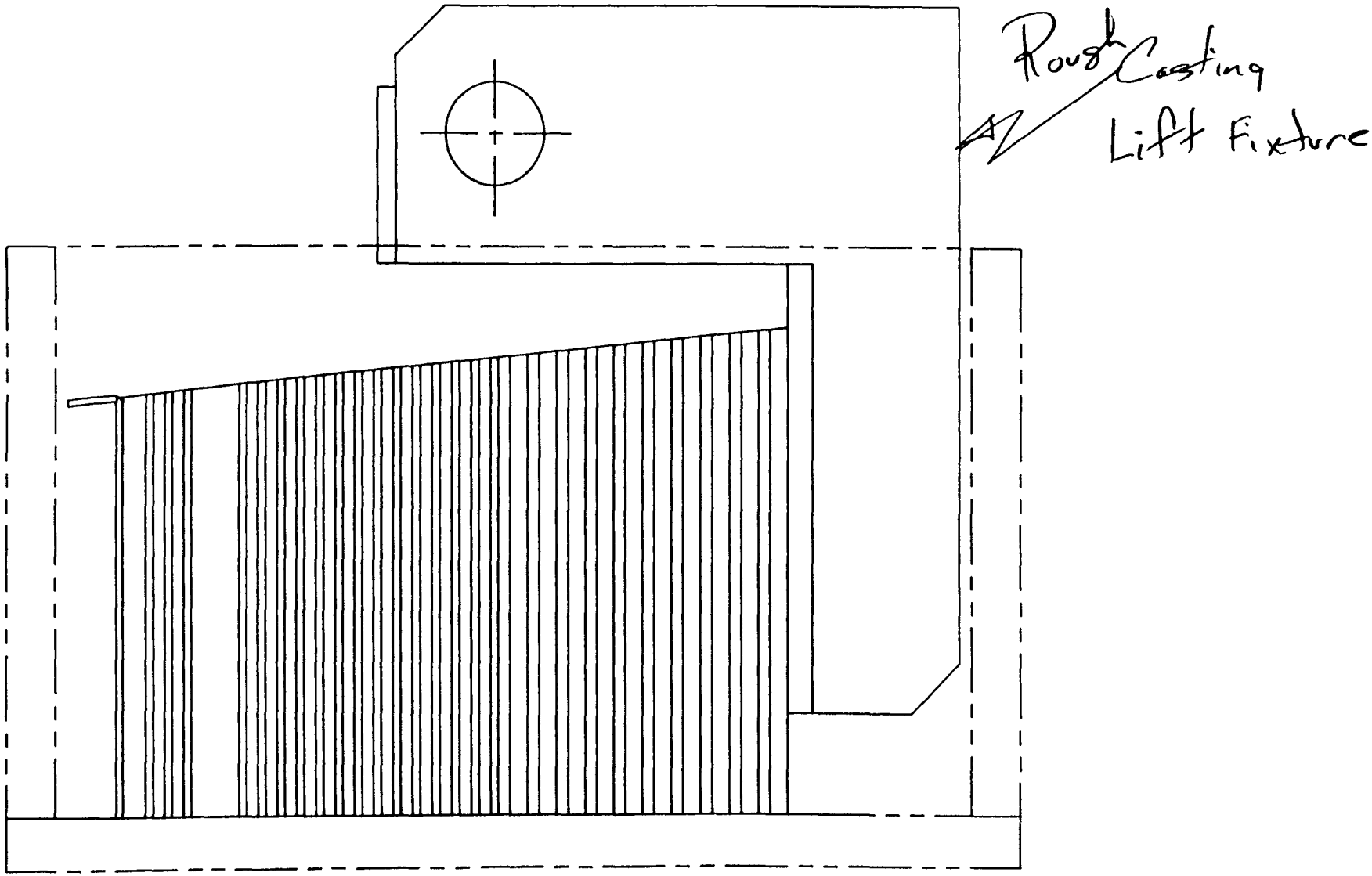

Figure 10

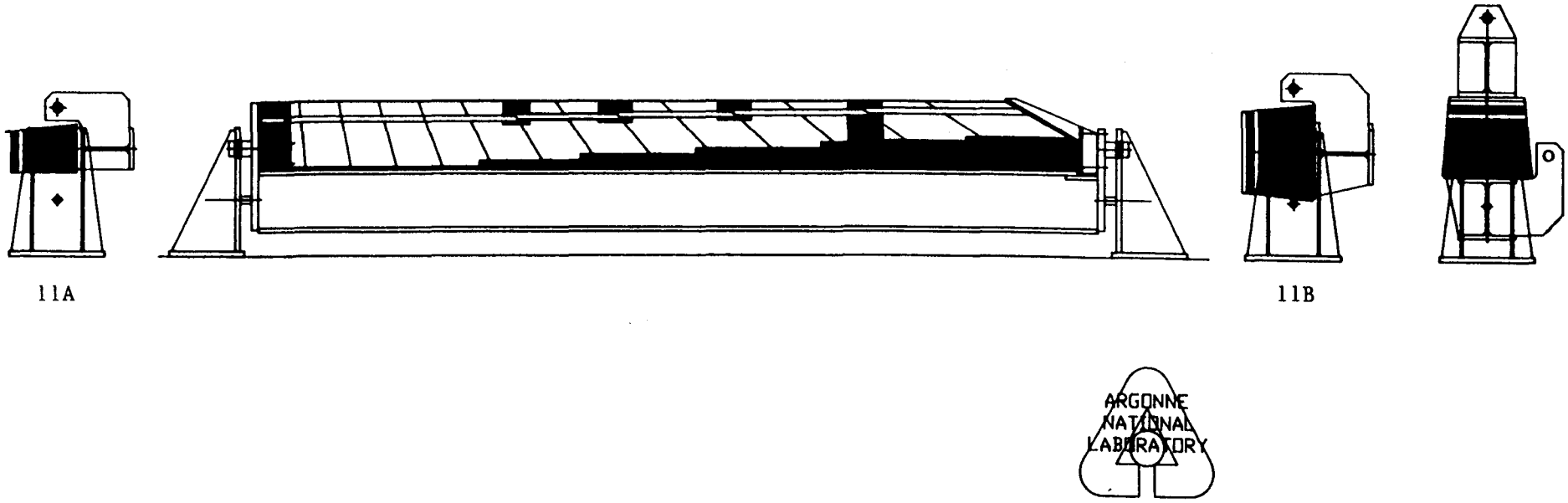

EM Handling and Rotating Fixture

Figure 11

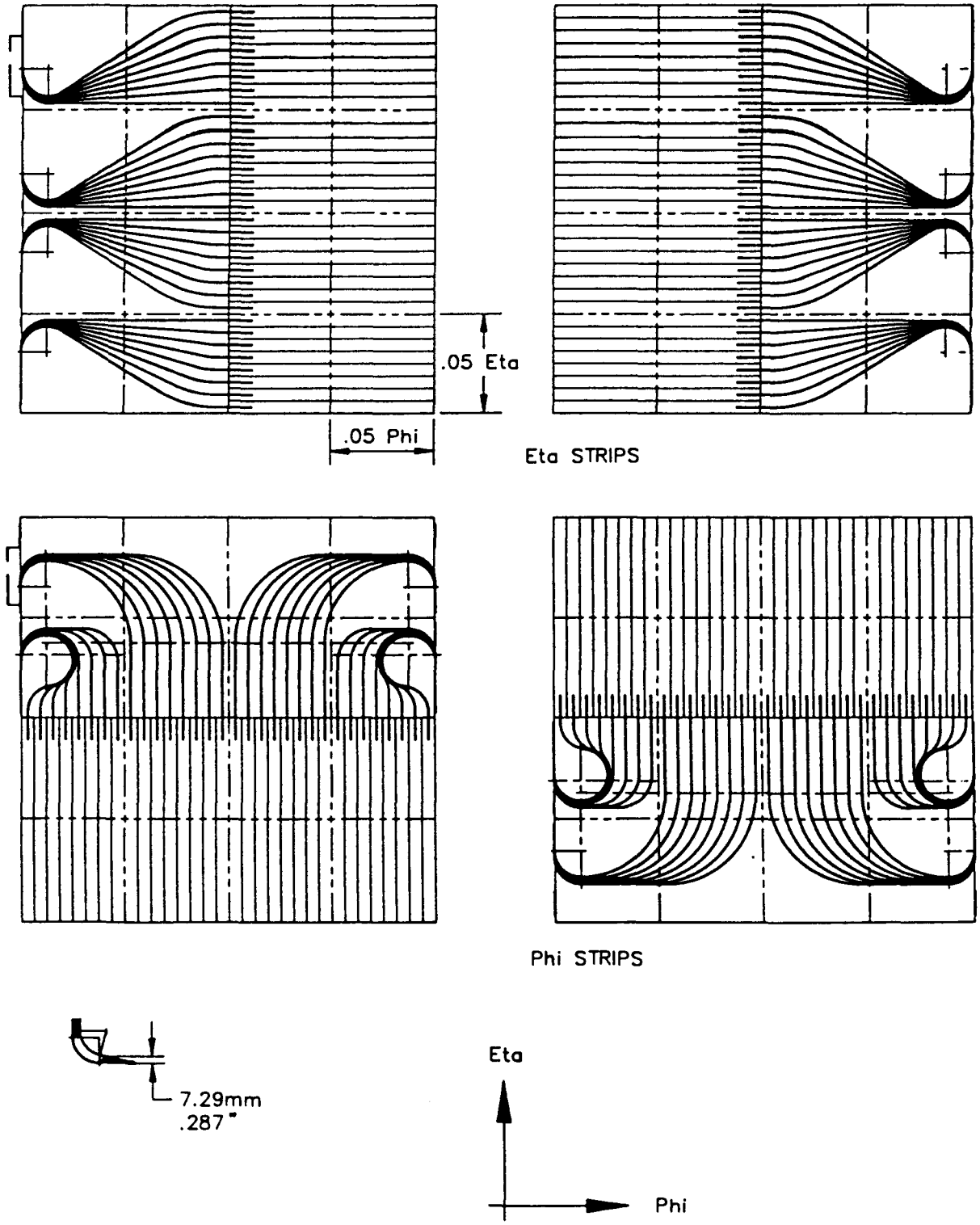

Figure 12

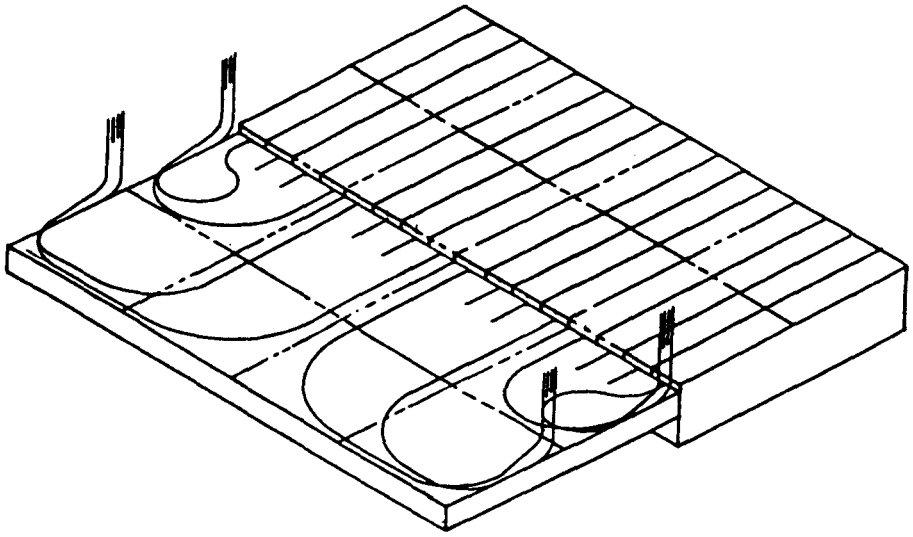

ϕ STRIPS

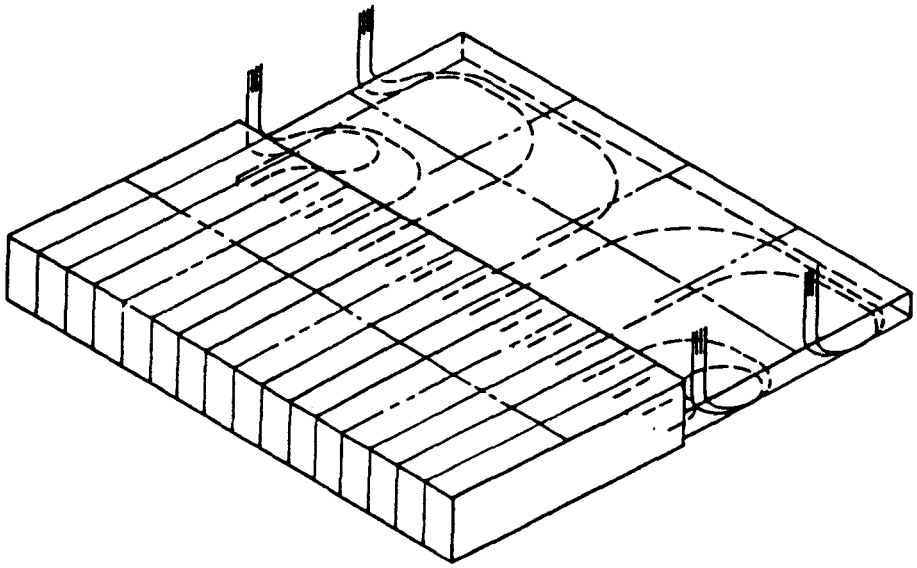

Figure 13

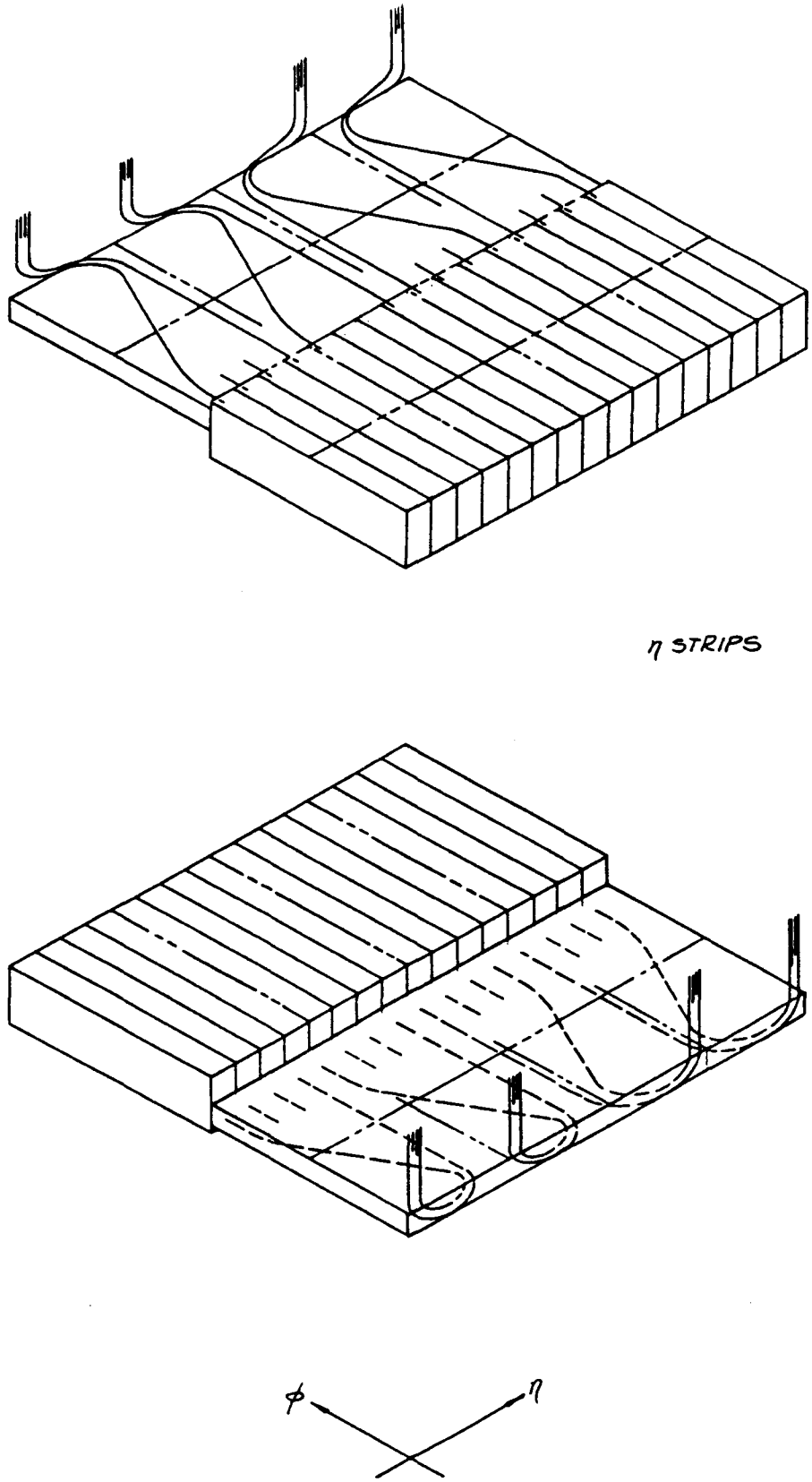

Figure 14

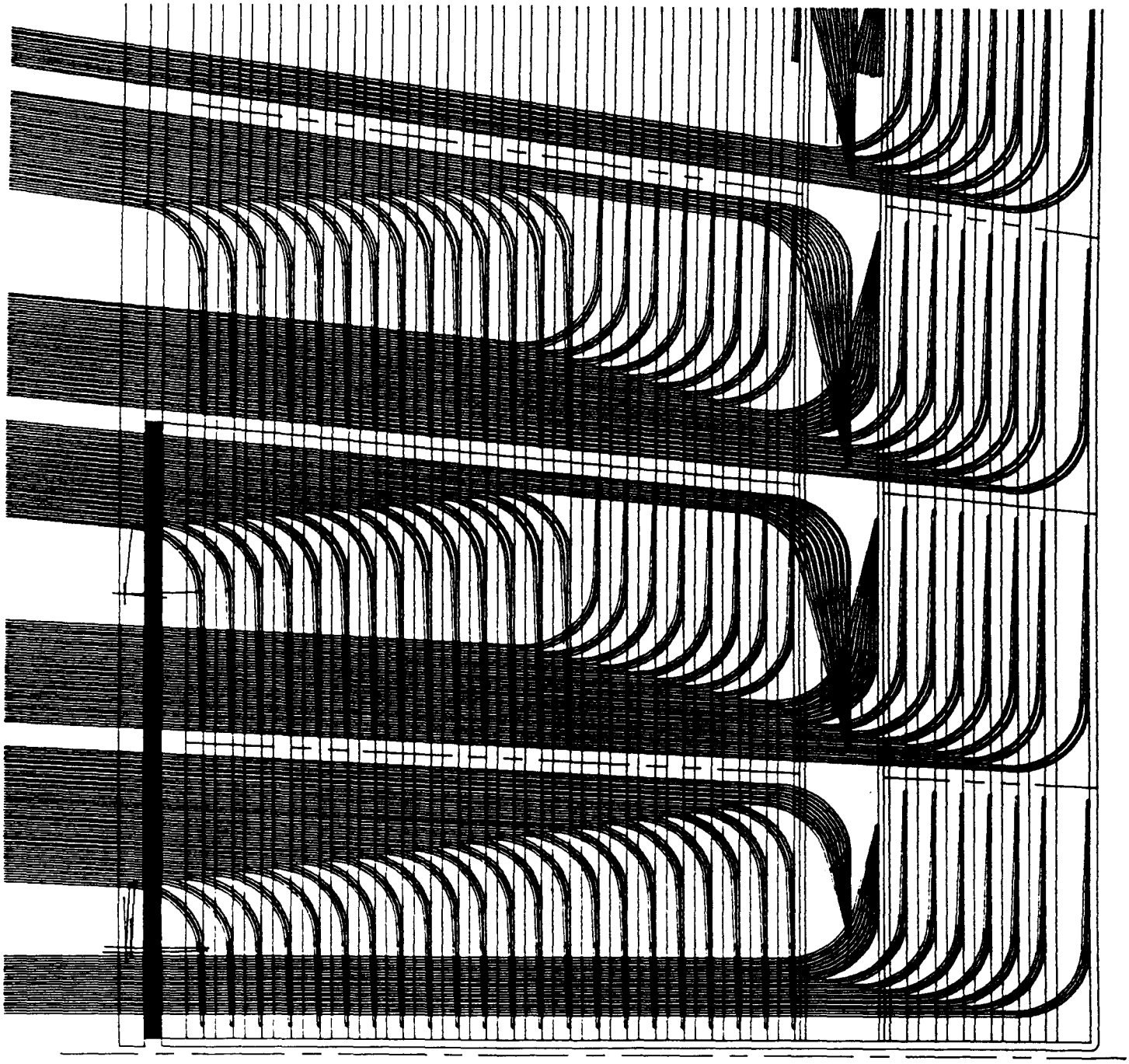

Figure 15

MOMENT vs. BULKHEAD DEFL.

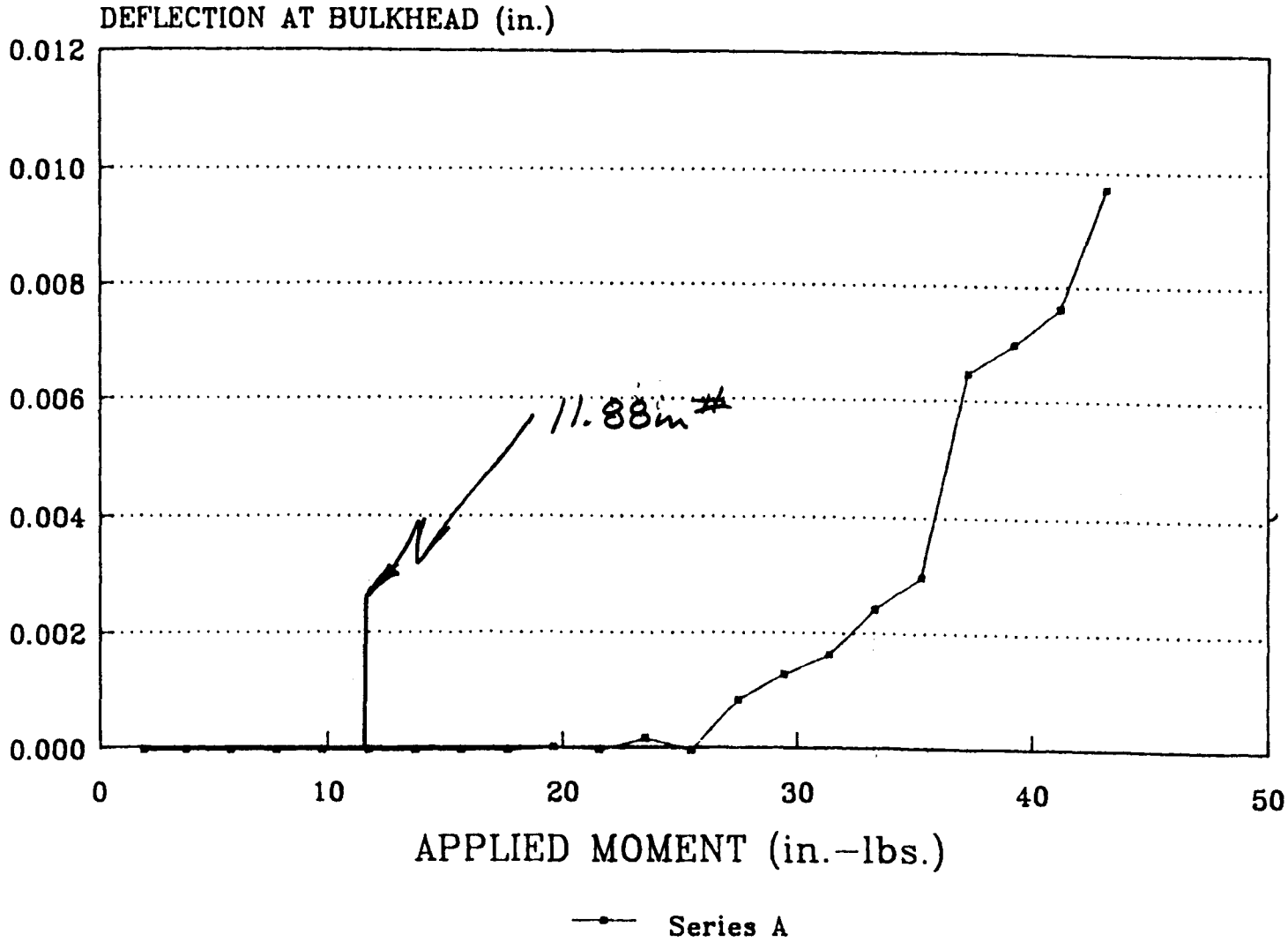

Figure 16

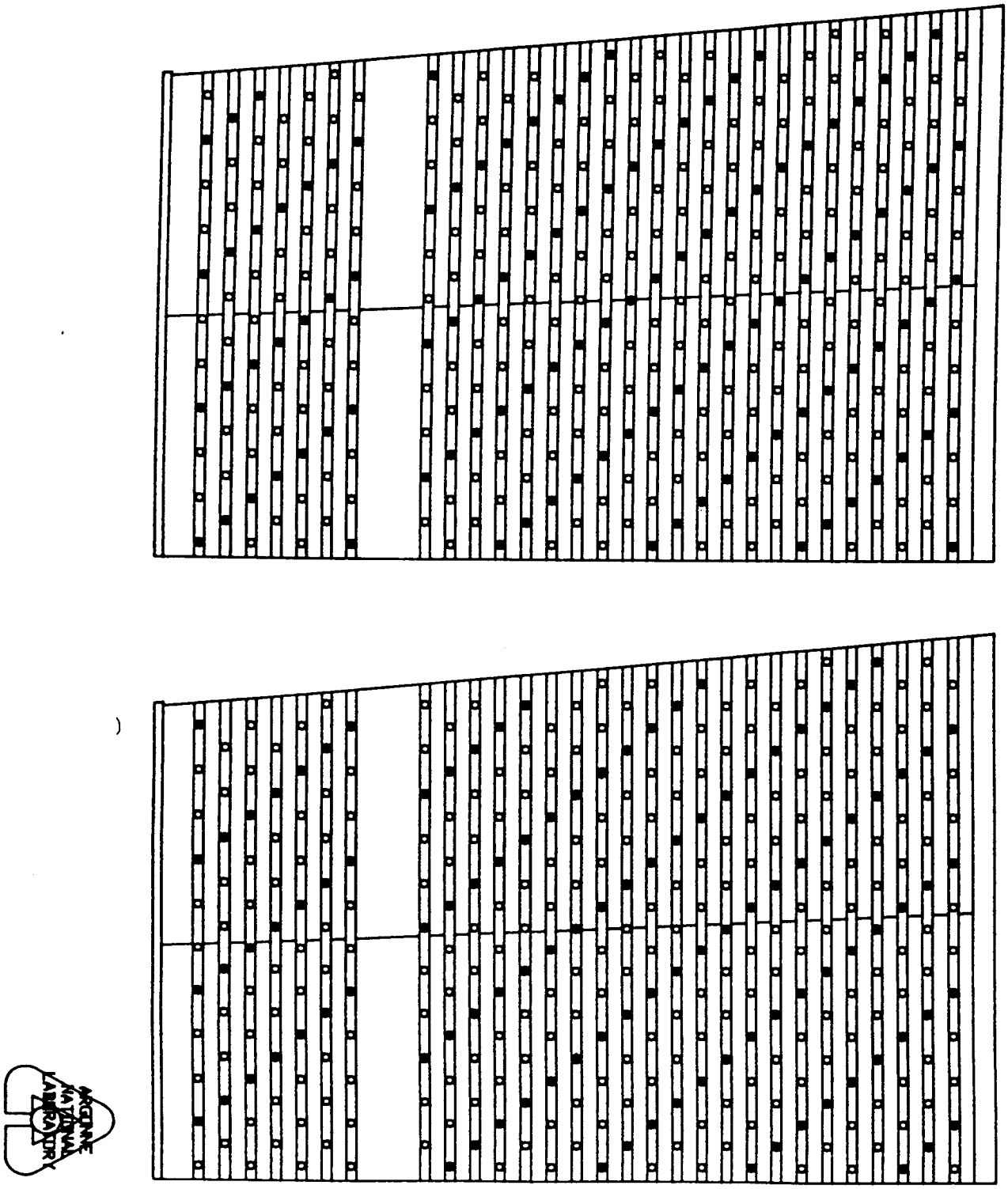

Figure 17

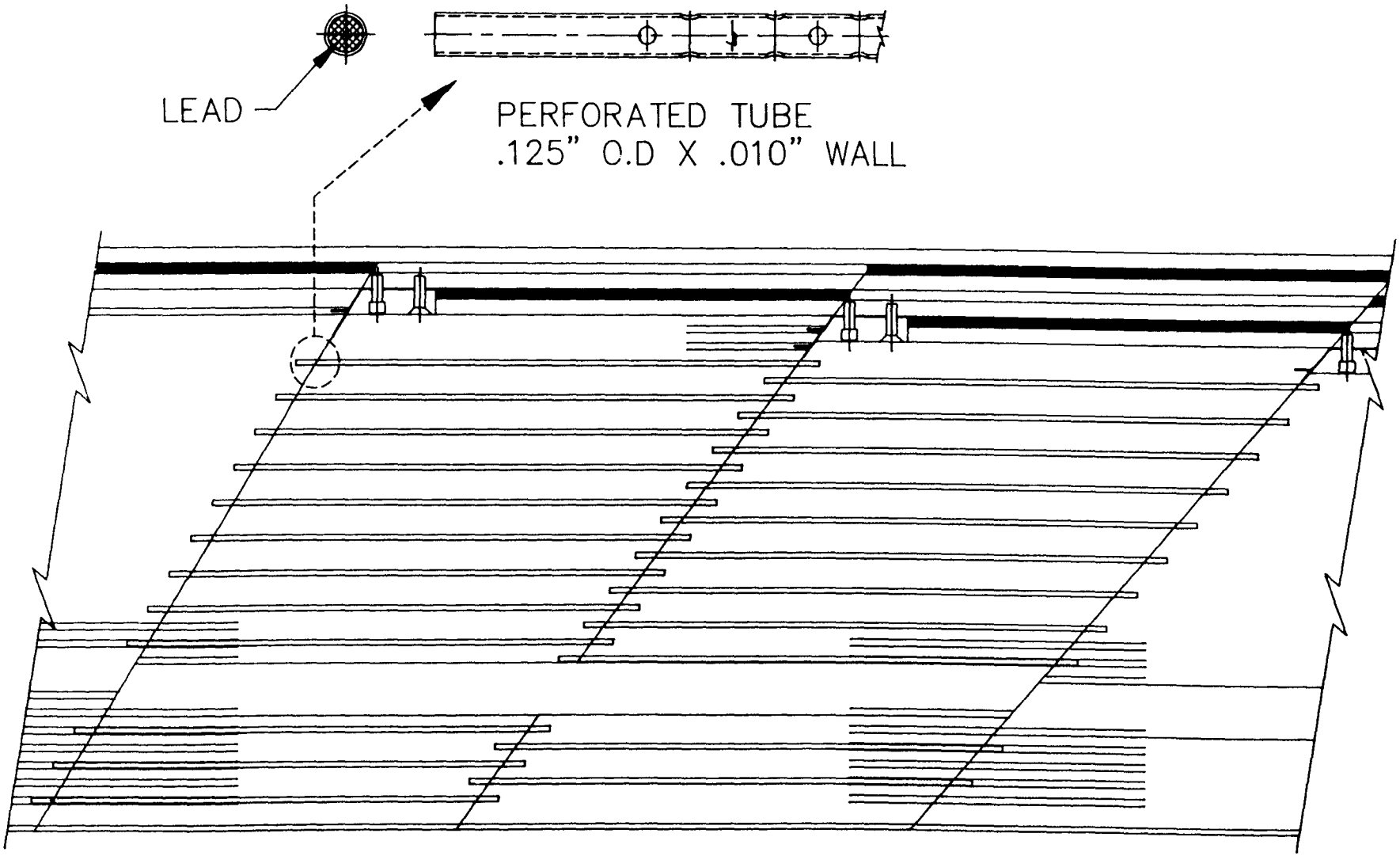

Figure 18

N 7/30/92

LEAD TUBE CALCULATIONS:

PROBLEM: WHAT IS THE σ & DEFLECTION OF A SERIES OF 4 PERFORATED TUBES WHEN THEY ARE UNDER LOADING FROM AN SDC LEAD SHEET?

TUBE DIA = .125"
WALL THICKNESS = .010"
LENGTH = 18.19" (LENGTH OF LONGEST Pb SHEET IN EM)

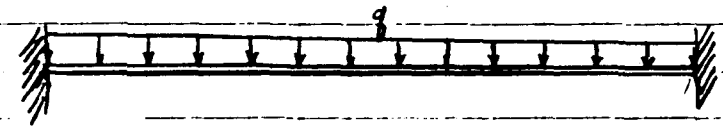

LOADING FROM Pb WEIGHT

1/64" 4mm

LEAD SHEET = (18.19") x (8.81") x (.1575")
VOLUME = 25.24 in^3
ρ_{Pb} = .411 lb/in^3
WEIGHT = 10.37#

EACH TUBE SEES 1/8 OF WEIGHT = 1.30#

q = WEIGHT/LENGTH = 1.30/18.19 = .0723 lb/IN

FROM ROARKE & YOUNG:

$M_{max} = qL^2/12$ AT BULKHEADS &
$M = qL^2/24$ AT MIDDLE OF SPAN

Figure 19

H ow TUBE ALONE

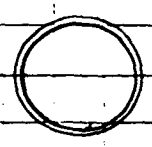

$\sigma = MY/I$

$M = qL^2/12$
$= (.0773)(18.19)^2/12$
$= 7.965$ in-lb

$I = \pi/4\,(R_2^4 - R_1^4)$
$= (\pi/4)(.0625^4 - .0525^4)$
$= (\pi/4)(7.662 \times 10^{-6})$
$= 6.017 \times 10^{-6}$ in^4

$\sigma = MY/I$
$= (7.965)(.063)/6.017 \times 10^{-6}$
$= 20{,}409$ psi

LEAD FILLED TUBE (COMPOSITE SECTION)

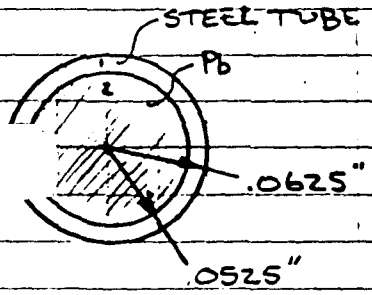

USING TRANSFORMED-SECTION METHOD
(GERE & TIMOSHENKO)

$\sigma = MY/I_T$

WHERE I_T = TRANSFORMED MOMENT OF INERTIA
$= I_2 + NI_1$

$N = E_1/E_2$
$I_1 = I_{\text{STEEL TUBE}}$
$I_2 = I_{\text{Pb 'ROD'}}$

$N = E_1/E_2 = 30 \times 10^6 / 3 \times 10^6 = 10$

$I_1 = 6.017 \times 10^{-6}$ in^4

$I_2 = \pi R_2^4/4$
$= \pi(.0525^4)/4$
$= 5.966 \times 10^{-6}$ in^4

$I_T = I_2 + NI_1$
$= (5.966 \times 10^{-6}) + (10)(6.017 \times 10^{-6})$
$= 6.6137 \times 10^{-5}$ in^4

$\sigma_T = MY/I_T$
$= (1.965)(.0625)/6.6137 \times 10^{-5}$
$= 2{,}856.85$ psi
→ AT OUTSIDE OF STEEL TUBE

$\sigma = MY/I$
$= (1.965)(.0525)/6.6137 \times 10^{-5}$
$= 1{,}559.75$ psi
→ AT Pb/TUBE JOINT

Figure 20

Appendix A

Mechanical Analysis of EM Calorimeter Module

Introduction

This report documents the results of a finite element mechanical analysis of a single, full size module of the electromagnetic (EM) calorimeter. This analysis was performed by the Westinghouse Science & Technology Center (WSTC) at the request of Argonne National Laboratory (ANL). The major objective was for WSTC to corroborate the analysis results obtained by ANL. This report summarizes the finite element model used by WSTC, and the results obtained from this model.

Description of Model

The current ANL design was used to make a finite element model. All major features of the design were incorporated in the model. The module has a rapidity span of 0-1.4, a length of 4.39 meters, and an azimuthal span of 0.1 (i.e., 1/64 of a circle, or 5.625°). Bulkheads are 0.5 mm thick stainless steel and are placed at rapidity intervals of 0.1. Every other bulkhead is interrupted at shower max, thus producing slots of $\lambda = 0.2$ at shower max, and slots of $\lambda = 0.1$ elsewhere. All bulkheads project through the interaction point. The radial position of the shower max slot is staggered per the ANL design. The front and side plates are 3.175 mm thick stainless steel. All lead alloy plates are 4 mm thick and have a modulus of 20,667 MPa (3 MPsi).

The geometry and material properties used in the model are listed in Tables 1, 2 and 3. The model as seen in the plane of the beamline is shown in Figure 1.

A full size EM module was modeled in ANSYS with four-node shell elements connected in an egg crate pattern in which the horizontal elements represent the steel front plate and the lead plates. The vertical and projective elements are the steel bulkheads, and thicker steel side plates.

Figure 1 shows the undeformed view of the model looking in the azimuthal direction. All the line segments shown in this figure represent the center planes of the lead and steel plate elements. The node and element mesh is created by sweeping this pattern (dragging in ANSYS parlance) in the azimuthal direction so that each line segment generates five shell elements over a span of 224 mm. The modeling was simplified by not representing the radial taper of the module. Thus, all elements are rectangular and have an azimuthal dimension of 44.8 mm.

Summary of WSTC Results

Corroboration between two analyses can be easily obtained by a visual inspection of the overall deflection plots and by comparing the magnitude of deflections and reaction forces at certain key points. The results of the WSTC analysis are summarized in this section.

The deflection of the steel frame in the 12 o'clock position is shown in Fig. 2. A maximum steel frame deflection of 1.66 mm occurs in the front plate at $\eta = 1.3$. this pattern of deflection occurs at all the odd numbered bulkhead connections, but gets progressively smaller as η decreases. At $\eta = 0.1$, the front plate deflection is 0.54 mm. The deflection at this point is strongly influenced by the boundary condition placed at the lower left corner. At this corner (R = 2100 mm, Z = 0), the end of the front plate is fixed in Z. The reaction load at this point is 2982 Nt (870 lbs.) in Z.

In summary, four data items can be used to compare the results obtained by WSTC with those obtained by ANL. These four items are: 1) The overall deflection pattern is graphically illustrated in Fig. 2. 2) The maximum radial deflection in the steel frame is 1.66 mm. It occurs in the front plate $\eta = 1.3$. 3) The radial deflection in the front plate at $\eta = 0.1$ is 0.54 mm. 4) The reaction load at the Z = 0 end of the front plate is 2982 Nt. (670 lbs.) in Z.

Table 1. Bulkhead Geometry for EM lead Casting 7-29-92

BULKHEAD NO.	bulkhead angle (RAD)	bulkhead angle (DEG)	Matl	THK (MM)	modulus (Mpsi)	R1 (MM)	R2 (MM)	Z1 (MM)	Z2 (MM)	BULKHEAD INTERRUPTIONS
0	1.5708	90.0001	st.steel	3.175	29	2101.5875	2425.175	2.5875	2.5875	NONE
1	1.4710	84.2800	st.steel	0.5	29	2101.5875	2425.175	210.5092	242.9219	PLATES 8-11
2	1.3721	78.6165	st.steel	0.5	29	2101.5875	2425.175	423.1252	488.275	NONE
3	1.2752	73.0635	st.steel	0.5	29	2101.5875	2425.175	639.976	738.515	PLATES 8-11
4	1.1811	67.6695	st.steel	0.5	29	2101.5875	2425.175	863.232	996.1463	NONE
5	1.0904	62.4762	st.steel	0.5	29	2101.5875	2425.175	1095.127	1263.747	PLATES 8-11
6	1.0039	57.5170	st.steel	0.5	29	2101.5875	2395.175	1337.983	1524.897	NONE
7	0.9218	52.8167	st.steel	0.5	29	2101.5875	2395.175	1594.23	1816.941	PLATES 7-10
8	0.8446	48.3916	st.steel	0.5	29	2101.5875	2365.175	1866.432	2100.526	NONE
9	0.7723	44.2504	st.steel	0.5	29	2101.5875	2365.175	2157.315	2427.892	PLATES 6-9
10	0.7050	40.3951	st.steel	0.5	29	2101.5875	2335.175	2469.788	2744.3	NONE
11	0.6427	36.8222	st.steel	0.5	29	2101.5875	2335.175	2806.98	3118.971	PLATES 5-8
12	0.5851	33.5240	st.steel	0.5	29	2101.5875	2305.175	3172.265	3479.573	NONE
13	0.5321	30.4894	st.steel	0.5	29	2101.5875	2305.175	3569.299	3915.069	PLATES 4-7
14	0.4835	27.7052	st.steel	3.175	29	2101.5875	2305.175	4002.056	4389.748	NONE

Table 2. Plate Geometry in EM Lead Casting 7-29-92

Plate No.	R of Center (mm)	Thk (mm)	Matl	modulus (Mpsi)	Z at left end (mm)	Z coordinate right end (mm)	Bulkhead No. at right end	bulkhead angle (RAD)	bulkhead angle (DEG)
1	2101.5875	3.175	st.steel	29	2.5875	4002.0562	14	0.4835	27.7052
2	2117.175	4	lead	3	2.5875	4031.7395	14	0.4835	27.7052
3	2127.175	4	lead	3	2.5875	4050.7825	14	0.4835	27.7052
4	2137.175	4	lead	3	2.5875	4069.8256	14	0.4835	27.7052
5	2147.175	4	lead	3	2.5875	4088.8686	14	0.4835	27.7052
6	2157.175	4	lead	3	2.5875	4107.9116	14	0.4835	27.7052
7	2167.175	4	lead	3	2.5875	4126.9546	14	0.4835	27.7052
8	2177.175	4	lead	3	2.5875	4145.9976	14	0.4835	27.7052
9	2187.175	4	lead	3	2.5875	4165.0406	14	0.4835	27.7052
10	2197.175	4	lead	3	2.5875	4184.0837	14	0.4835	27.7052
11	2207.175	4	lead	3	2.5875	4203.1267	14	0.4835	27.7052
12	2217.175	4	lead	3	2.5875	4222.1697	14	0.4835	27.7052
13	2227.175	4	lead	3	2.5875	4241.2127	14	0.4835	27.7052
14	2237.175	4	lead	3	2.5875	4260.2557	14	0.4835	27.7052
15	2247.175	4	lead	3	2.5875	4279.2987	14	0.4835	27.7052
16	2257.175	4	lead	3	2.5875	4298.3417	14	0.4835	27.7052
17	2267.175	4	lead	3	2.5875	4317.3848	14	0.4835	27.7052
18	2277.175	4	lead	3	2.5875	4336.4278	14	0.4835	27.7052
19	2287.175	4	lead	3	2.5875	4355.4708	14	0.4835	27.7052
20	2297.175	4	lead	3	2.5875	4374.5138	14	0.4835	27.7052
21	2307.175	4	lead	3	2.5875	3482.5915	12	0.5851	33.5240
22	2317.175	4	lead	3	2.5875	3094.9289	11	0.6427	36.8222
23	2327.175	4	lead	3	2.5875	3108.2854	11	0.6427	36.8222
24	2337.175	4	lead	3	2.5875	2746.6508	10	0.7050	40.3951
25	2347.175	4	lead	3	2.5875	2409.4144	9	0.7723	44.2504
26	2357.175	4	lead	3	2.5875	2419.6796	9	0.7723	44.2504
27	2367.175	4	lead	3	2.5875	2102.3023	8	0.8446	48.3916
28	2377.175	4	lead	3	2.5875	1803.2862	7	0.9218	52.8167
29	2387.175	4	lead	3	2.5875	1810.8720	7	0.9218	52.8167
30	2397.175	4	lead	3	2.5875	1526.1701	6	1.0039	57.5170
31	2407.175	4	lead	3	2.5875	1254.3676	5	1.0904	62.4762
32	2417.175	4	lead	3	2.5875	1259.5785	5	1.0904	62.4762

Table 3. Shower Max Slot Location 7–29–92

Tower No.	Bulkhead No. at left end	Bulkhead No. at right end	Lead Plates Omitted for Shower Max Slot
1	0	1	Plate Nos. 9 & 10
2	1	2	Plate Nos. 9 & 10
3	2	3	Plate Nos. 9 & 10
4	3	4	Plate Nos. 9 & 10
5	4	5	Plate Nos. 9 & 10
6	5	6	Plate Nos. 9 & 10
7	6	7	Plate Nos. 8 & 9
8	7	8	Plate Nos. 8 & 9
9	8	9	Plate Nos. 7 & 8
10	9	10	Plate Nos. 7 & 8
11	10	11	Plate Nos. 6 & 7
12	11	12	Plate Nos. 6 & 7
13	12	13	Plate Nos. 5 & 6
14	13	14	Plate Nos. 5 & 6

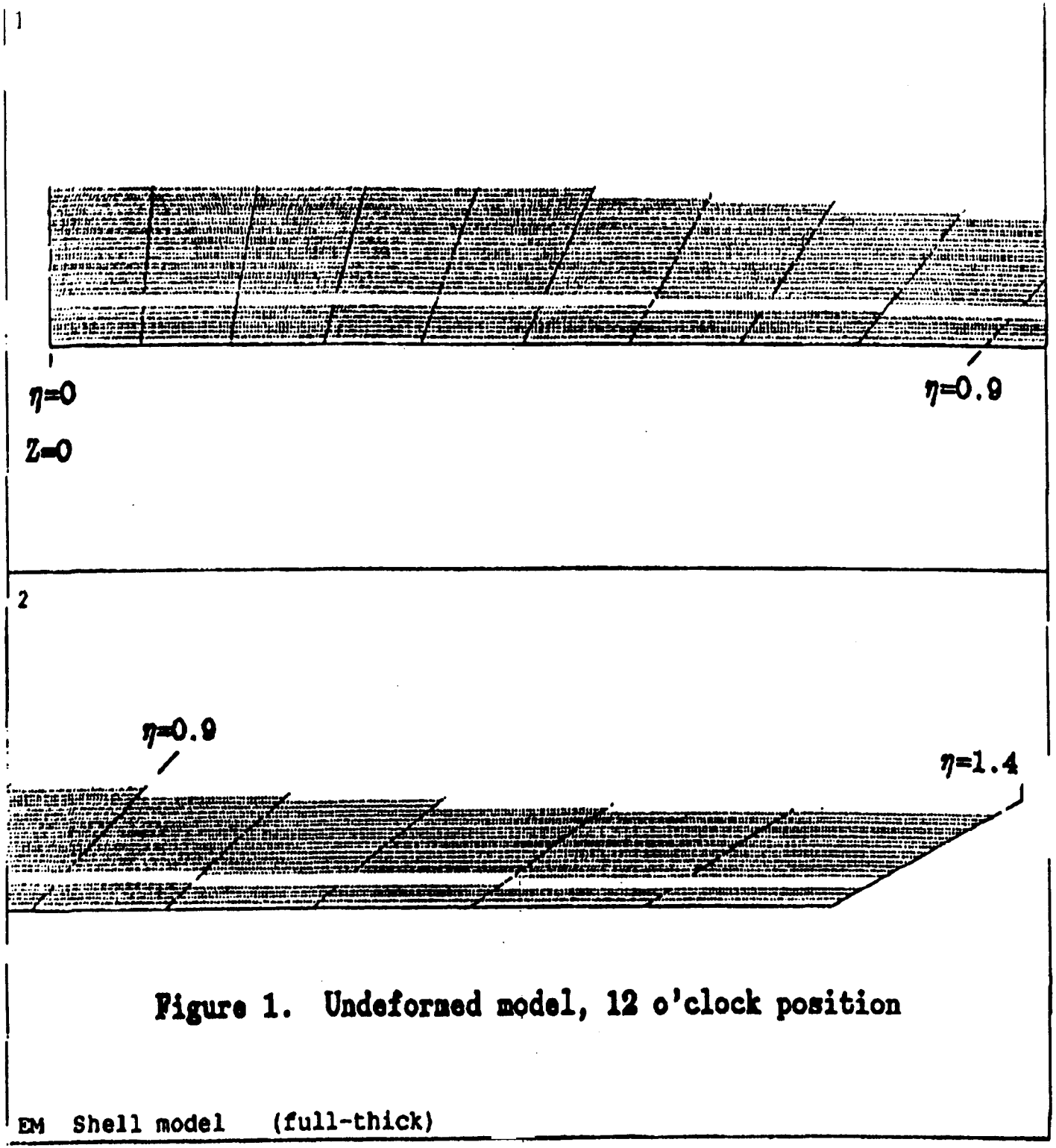

ANSYS 4.4A1
JUL 21 19
19:35:18
PLOT NO. 1
PREP7 ELEMENTS
TYPE NUM

YV =1
*DIST=600
*XF =2222
*YF =111
*ZF =1100
VUP =X

WIND=2
YV =1
*DIST=600
*XF =2222
*YF =111
*ZF =3300
VUP =X

Figure 1. Undeformed model, 12 o'clock position

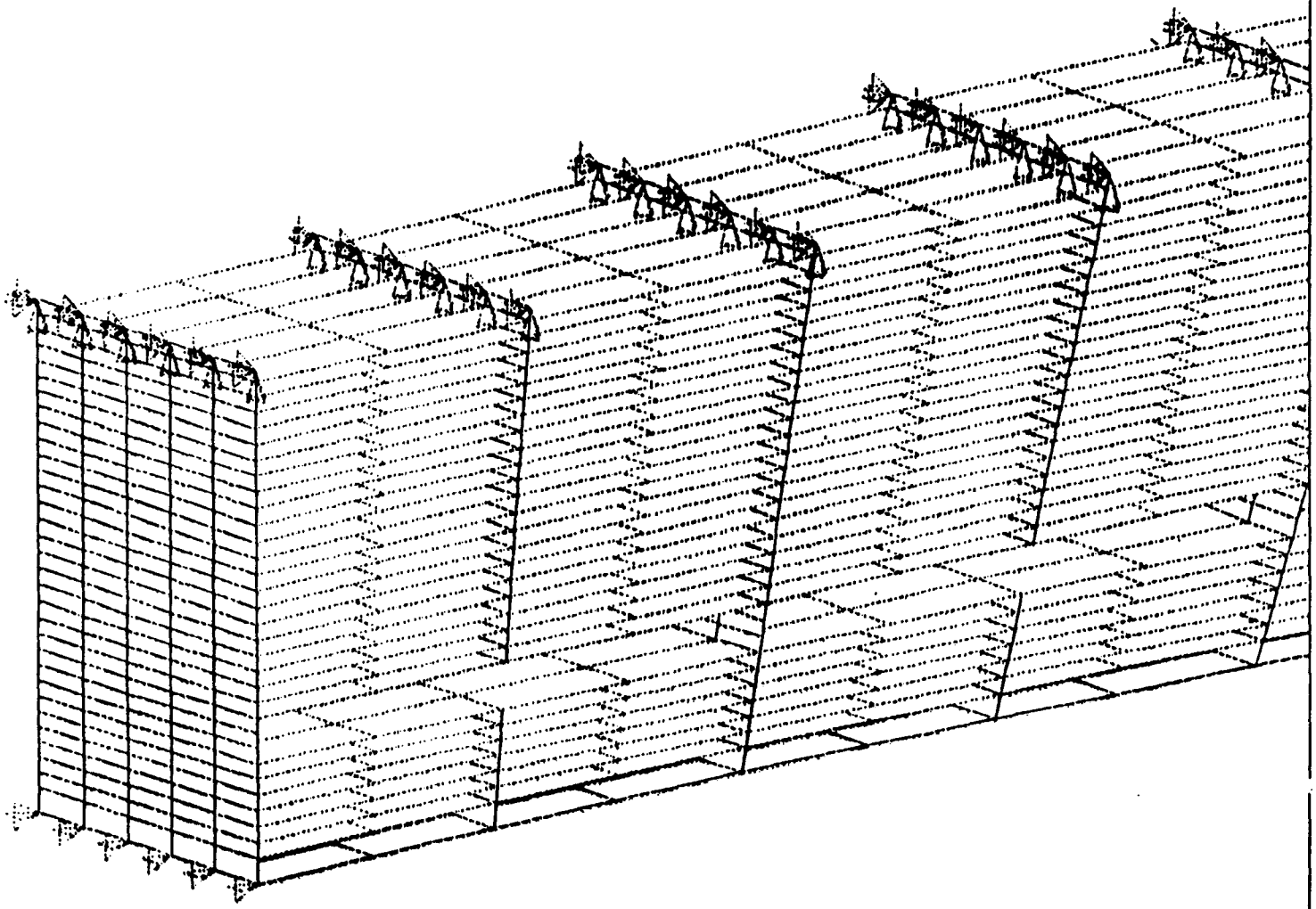

JUL 21 1992
21:05:22
PLOT NO. 1
PREP7 ELEMENTS
TYPE NUM
TDIS

XV =1
YV =3
ZV =-2.5
*DIST=440
*XF =2250
*YF =111
*ZF =430
VUP =X
PRECISE HIDDEN

EM She odel (full-thick)

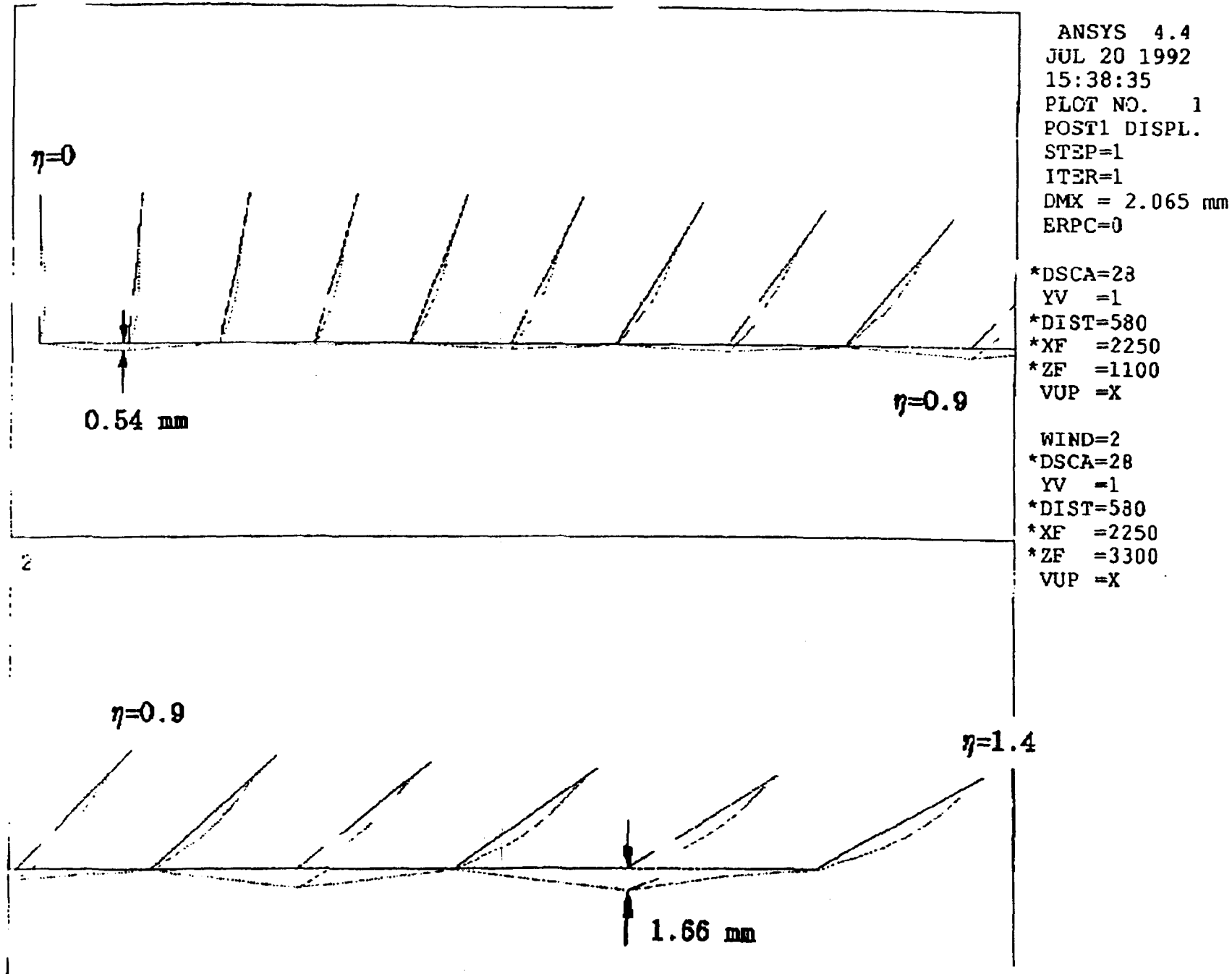

Figure 2. Deformed model, 12 o'clock position

1

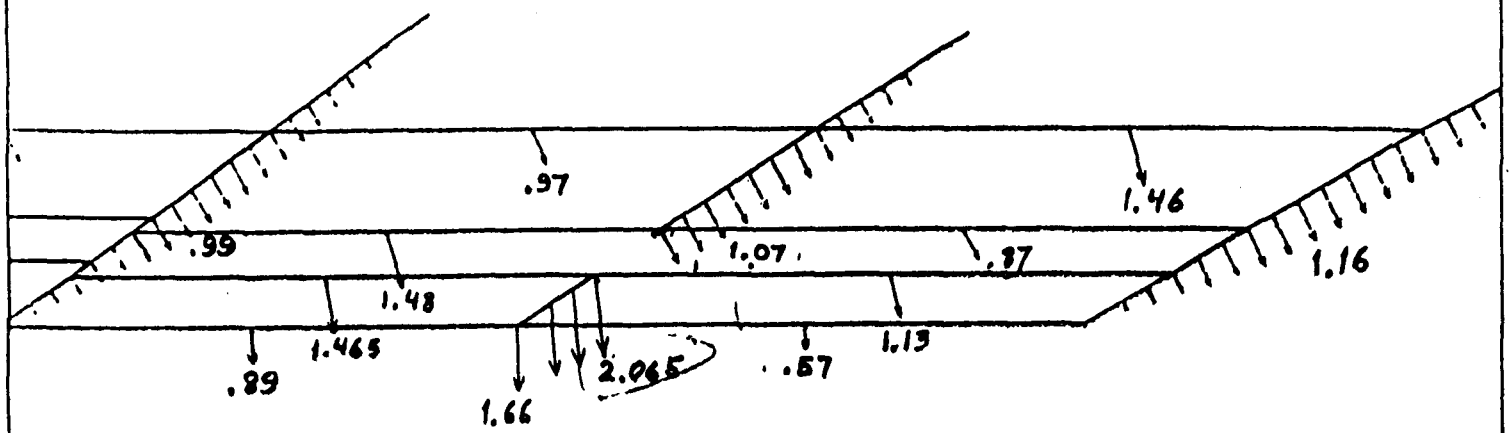

JUL 21 1992
16:41:50
PLOT NO. 1
POST1 VECTOR
STEP=1
ITER=1
DISP
NODE=1033
0.229406 mm
0.458811
0.688217
0.917622
1.147
1.376
1.606
1.835
2.065 mm

YV =1
*DIST=570
*XF =2222
*YF =111
*ZF =3750
VUP =X

FM Shell Model (full-thick) 12 o'clock

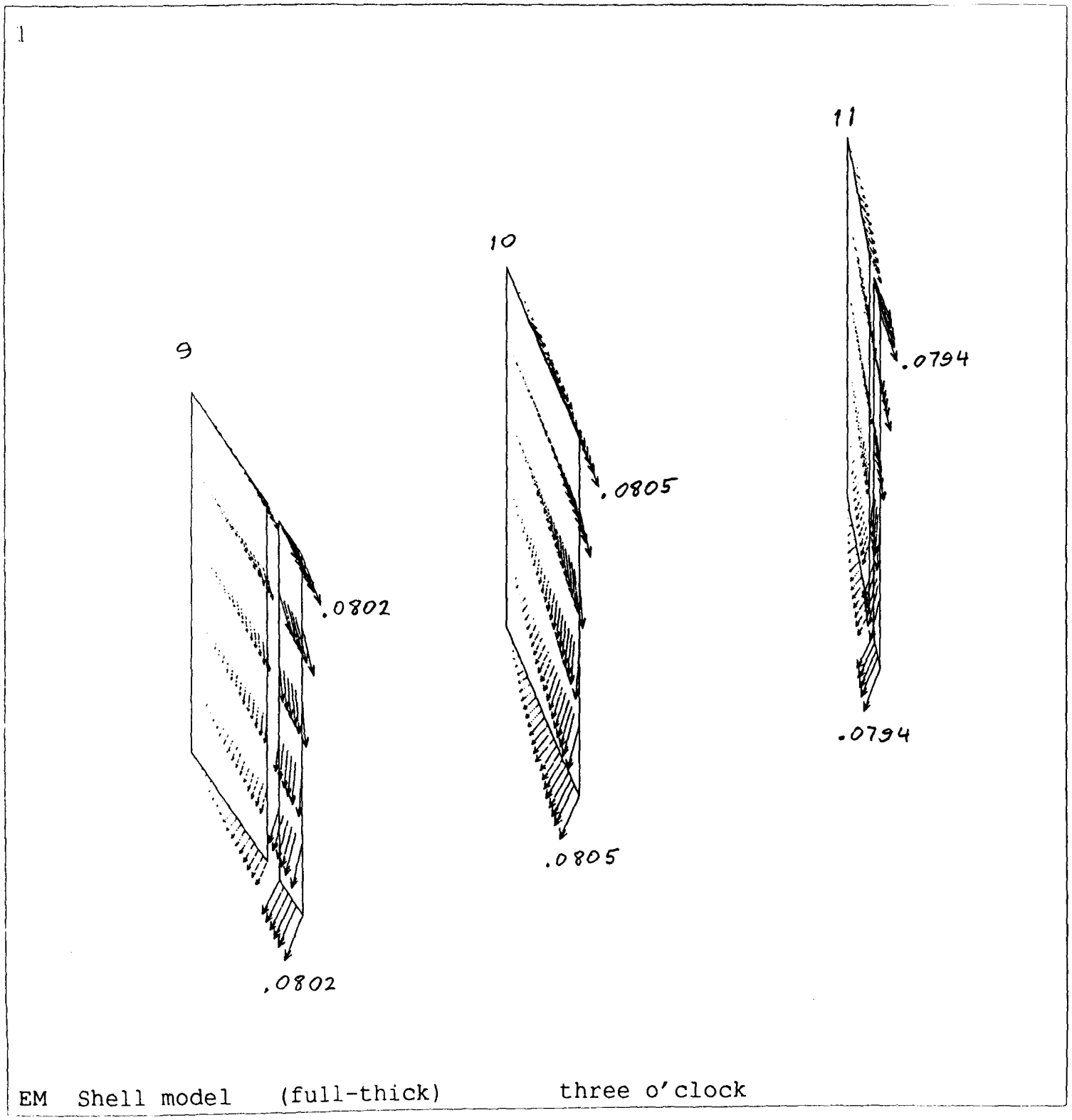

EM Shell model (full-thick) three o'clock

ANSYS 4.4A1
JUL 21 1992
22:35:18
PLOT NO. 1
POST1 ELEMENTS
TYPE NUM

XV =1
YV =2
ZV =-3
*DIST=330
*XF =100
*YF =-2222
*ZF =2600
VUP =X
EDGE

POST1 VECTOR
STEP=1
ITER=1
DISP
NODE=850
0.008945 mm
0.01789
0.026834
0.035779
0.044724
0.053669
0.062614
0.071558
0.080503 mm

XV =1

1

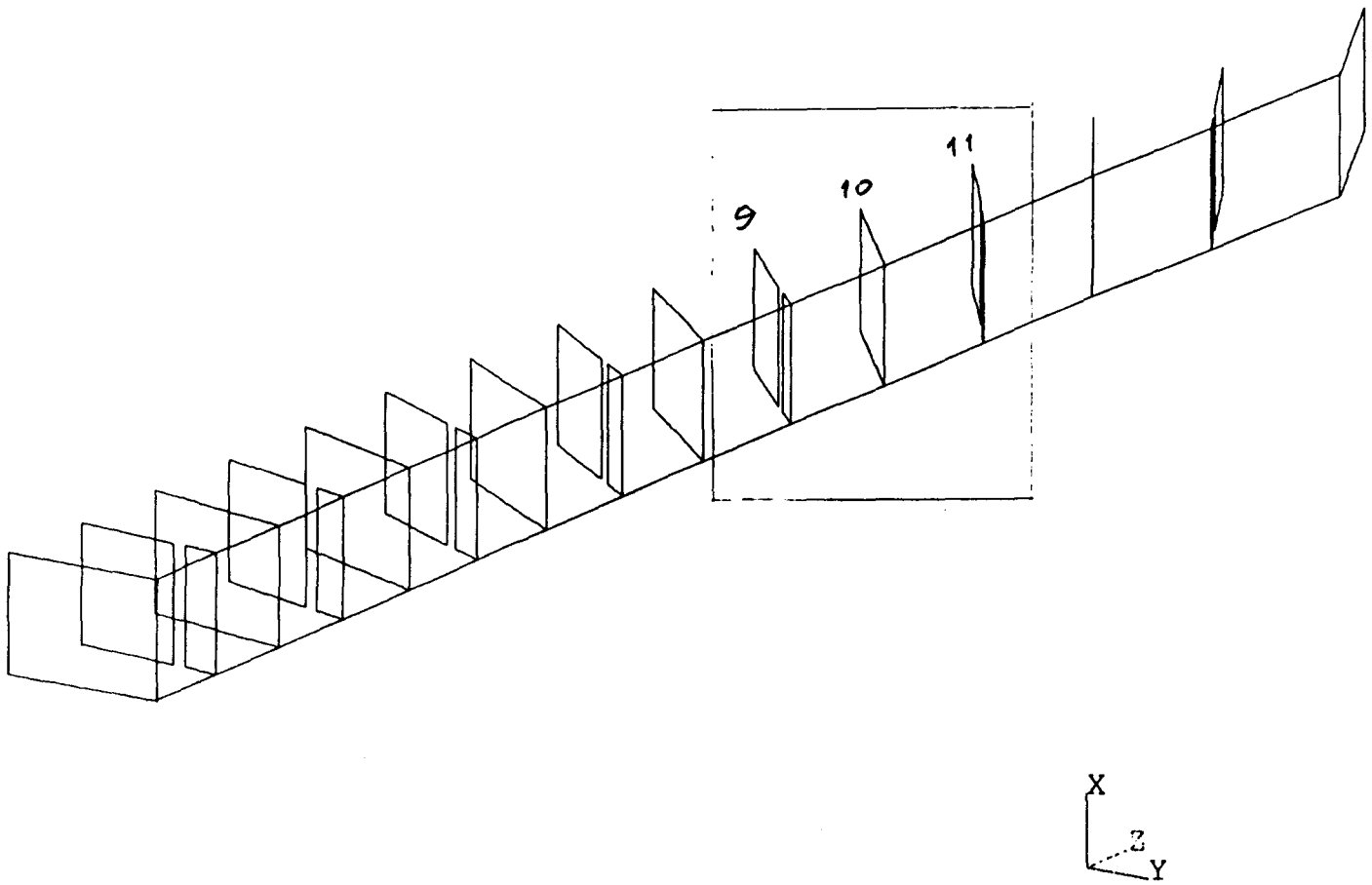

ANSYS 4.4A1
JUL 21 1992
22:39:55
PLOT NO. 1
POST1 ELEMENTS
TYPE NUM

XV =1
YV =2
ZV =-3
*DIST=1359
*XF =-86.41
*YF =-2470
*ZF =2373
VUP =X
EDGE

EM She model (full-thick) three o' :k